INTERFACIAL MECHANICAL PROPERTIES AT EQUILIBRIUM OF FUNCTIONALIZED ZnO QUANTUM DOTS MONOLAYERS AT THE AIR/WATER INTERFACE

PROPIEDADES MECÁNICAS INTERFACIALES EN EQUILIBRIO DE MONOCAPAS DE PUNTOS CUÁNTICOS DE ZnO EN LA INTERFASE AIRE/AGUA

L.M. Montes-de-Oca[1]* and A. Hernandez-Prudencio[2]

[1]*Instituto de Física y Matemáticas, Universidad Michoacana de San Nicolás de Hidalgo, Morelia, Michoacán, México*

[2]*Facultad de Ingeniería Química, Universidad Michoacana de San Nicolás de Hidalgo, Morelia, Michoacán, México.*

Abstract

In this work, the mechanical properties at equilibrium of two dimensional layers made by ZnO Quantum dots deposited at the air/water interface were studied. ZnO nanoparticles were synthesized by the sol-gel method and their functionalization was made by the hydrolytic silanization method. Their mechanical properties were evaluated using a Langmuir trough equipped with a Du Noüy-Padday rod. With this technique, isotherms, compression modules and hysteresis cycles of the system were obtained. Our results showed that partially hydrophobic particles form two dimensional soft solids at the air/water interface, reaching values of their adiabatic compression modulus corresponding to a liquid condensed phase when they are compressed above surface concentrations of the order of 1×10^1 mg/m^2. Nanoparticle layers presented dependence with the rate of compression and significant hysteresis, showing their complex behavior. Layers did not present collapse, but a semi constant value of the pressure upon high surface concentrations was observed, an indicative of the high adsorption energy of the nanoparticles. The mechanical properties reported, make these particles suitable for further applications on the stabilization of aqueous foams.

Keywords: ZnO, Quantum dot, particle monolayer, isotherms, compression modulus.

Resumen

En este trabajo se estudiaron las propiedades mecánicas en el equilibrio de membranas bidimensionales formadas por puntos cuánticos de ZnO, depositados en la interfaz aire/agua. Las nanopartículas fueron sintetizadas por el método de sol-gel y se realizó su funcionalización por el método de silanización hidrolítica. Se evaluaron sus propiedades mecánicas usando una palangana de Langmuir equipada con un rodillo de Du Noüy-Padday. Con esta técnica, se obtuvieron las isotermas, módulos de compresión y ciclos de histéresis del sistema. Nuestros resultados muestran que las partículas parcialmente hidrofóbicas forman sólidos suaves bidimensionales en la interfaz aire/agua, alcanzando valores de sus módulos de compresión adiabática correspondientes a una fase líquida condensada cuando son comprimidos sobre concentraciones superficiales del orden de 1×10^1 mg/m^2. Las membranas formadas por las nanopartículas presentaron dependencia con la razón de compresión a la vez que una histéresis significativa, demostrando su comportamiento complejo. Las membranas no presentaron colapso, en lugar de ello, se observó un valor semi-constante de la presión a altas concentraciones superficiales, un indicativo de la alta energía de adsorción de las nanopartículas. Las propiedades mecánicas reportadas hacen de estas nanopartículas, candidatas adecuadas para futuras aplicaciones en la estabilización de espumas acuosas.

Palabras clave: ZnO, puntos cuánticos, monocapa de partículas, isotermas, módulo de compresión.

1 Introduction

In the last decades, efforts had been conducted in the development and characterization of coloidal systems stabilized with organic or inorganic non-toxic or materials, including, for example, the stabilization of foams by proteins (Rodríguez-Huezo, Villagcheómez-Zavala, Lozano-Valdés, & Pedroza-Islas, 2010), the formation of multiple emulsions stabilized by Mesquite (*Prosopis laevigata*) Gum-chitozan mixtures (Perez, Barrios, Roman, & Pedroza, 2011), by milk fat globule membrane(Olivarez-Romero, Faustino-vega, E., González-Vázquez, & Azaola-Espinosa, 2018) and by xanthan gum, guar gum and locust bean gum (Pavón-García *et al*., 2014).

Among the wide variety of colloidal systems, foams and emulsions stabilized by solid particles are of great interest due to their industrial applications. Particles can be used as stabilizers in situations where surfactants cannot, as in systems exposed to high temperatures. Even when solid particles has been widely exploited as stabilizers in Pickering emulsions (Aveyard, Binks, & Clint, 2003; Binks, 2002; Pickering, 1907), their adsorption to the gas-liquid interface and their ability to stabilize aqueous foams without using surfactants has been only recently studied (Binks, 2002; Du *et al*., 2003; Gonzenbach, Studart, Tervoort, & Gauckler, 2006; Safouane, Langevin, & Binks, 2007; Stocco, Garcia-Moreno, Manke, Banhart, & Langevin, 2011; D. Zang, Langevin, Binks, & Wei, 2010; D. Y. Zang, Rio, Langevin, Wei, & Binks, 2010). Of special interest is the use of particles whose size is on the order of nanometers (Gonzenbach *et al*., 2006; Safouane *et al*., 2007; D. Zang *et al*., 2010; D. Y. Zang *et al*., 2010), as this feature reduces the time required for the particles to diffuse and adsorb on the air/water interface, favoring the foam formation(Beneventi, Carre, & Gandini, 2001; Gonzenbach *et al*., 2006; Miller, Joos, & Fainerman, 1994). Another interesting feature of the use of particles to foam stabilization is that, since particles have high adsorption energies, of the order of thousands of kT (Aveyard *et al*., 2003; Du *et al*., 2003), it tends to stabilize foams by prolonged lifetimes, even of months (Arriaga *et al*., 2012; Gonzenbach *et al*., 2006; Stocco *et al*., 2011), or above(Cervantes Martinez *et al*., 2008). It is regarded that the colloidal film placed at the air/water interface of these foams, inhibit the bubble coalescence and coarsening; the main mechanisms of foam destabilization (Cervantes Martinez *et al*., 2008; Dickinson, 2010; Hunter, Pugh, Franks, & Jameson, 2008). To have a better understanding of the properties of particle stabilized foams, and to progress on their technological applications, it is needed the development of new functionalized materials using controlled procedures of synthesis and coating, and conducting the corresponding characterization of their mechanical properties at the air/water interface.

From the wide quantity of materials that can be surface functionalized for this purpose, Zinc Oxide (ZnO) was chosen, to be a non-toxic material with crystalline, well defined structure (Morkoç & Özgür, 2009; Özgür *et al*., 2016), also because its optical properties, as the stable emission and the presence of visible emission along an UV emission peak (Bang, Yang, & Holloway, 2006; Bera, Qian, Sabui, Santra,

& Holloway, 2008; Lv, Xiao, Li, Xue, & Ding, 2013; Van Dijken, Meulenkamp, Vanmaekelbergh, & Meijerink, 2000), and because this material is susceptible to be doped with other elements to have control on their optical properties (El Filali, Torchynska, Díaz Cano, & Morales Rodríguez, 2015). All these features can lead to new applications of nanoparticle stabilized foams. ZnO as quantum dots are nanostructures that takes a semispherical shape. It has been used in cell imaging (Li *et al*., 2015) and in selective detection of aldehydes (Jana, Yu, Ali, Zheng, & Ying, 2007). ZnO nanostructures can be synthesized by several methods, such as sol-gel (Benhebal *et al*., 2013), co-precipitation (Khan *et al*., 2018), by using microemulsion environment (Lavand & Malghe, 2018), by metallurgical process (Mahmud, Abdullah, Putrus, Chong, & Mohamad, 2006) and hydrothermal synthesis (Alshehri, Lewis, Pleydell-Pearce, & Maffeis, 2017). Among those methods, Sol-gel is particularly interesting due to its repeatability, low cost and simplicity (Kołodziejczak-Radzimska & Jesionowski, 2014).

In this work, ZnO nanoparticles were synthesized using the sol-gel method and their surface were further functionalized with trimethoxy(octadecyl)silane (ODS), to render them partially hydrophobic. Their mechanical properties at the air/water interface at equilibrium were studied using a Langmuir trough equipped with a Du Noüy-Padday rod. With this technique, isotherms, compression modules and hysteresis cycles were obtained and the behavior was discussed.

2 Materials and methods

2.1 Controlled synthesis of ZnO Qdots

ZnO nanoparticles were prepared by a sol-gel process from Zn acetate (Sigma) and NaOH (Sigma) as precursors, following a procedure similar to that reported in(Bera *et al*., 2008). For a typical synthesis, 0.002 mol of Zn acetate where dissolved in 30 ml of ethanol at 70 ºC and 0.005 mol of NaOH where dissolved in 30 ml of ethanol at 50-60 ºC so that, it has a $[OH^-]/[Zn^{2+}]$ ratio of 2.5. Both were dissolved with vigorous stirring. Then, the solutions were cooled to a low temperature. The Zn^{2+} solution was placed in an ice bath, whose temperature was controlled by a refrigerated/heated bath circulator (HAAKE A10, Thermo scientific). Once the Zn^{2+} solution reached

the desired temperature for the synthesis, the OH⁻ solution was added into the Zn^{2+} solution by dripping. Two syringes (20 mL, Beckton-Dickinson) were filled with the OH⁻ solution and the time of dripping was controlled using syringe pumps (Kent Scientific) with programmed flow ratios. ZnO Qdots were synthesized during 30 minutes at the temperature of 0 ℃ under vigorous stirring. In all cases, the temperature was kept constant during the total time of the synthesis. The resulting ZnO nanoparticles were precipitated by addition of n-heptane. The volume ratio of n-heptane to solution was 3:2. After centrifugation (at 3000 rpm during 10 minutes), the resulting precipitate was washed into 100 ml of ethanol. ZnO Qdots were washed three times with ethanol in order to remove acetate and sodium ions remnants. Finally, the resulting washed ZnO Qdots were dried in an oven at 40 ℃ during one day and stored. Then, the resulting powder was dispersed in ethanol to study their fluorescence.

2.2 Preparation of ZnO@ODS Nano-composites

The ZnO@ODS nanocomposites were obtained by coating the ZnO Qdots with the hydrophobic ODS layer by the hydrolytic silanization procedure in ethanol. 2% and 4% v/v solutions of ODS in a 1 mg/mL suspension of Qdots in ethanol were prepared. The mixture was stirred 1h at room temperature. The resultant ZnO@ODS nanocomposites were centrifuged and washed three times with ethanol. The resulting washed ZnO@ODS nanocomposites were dried in an oven at 40 ℃ during one day and stored. Then, they were redisposed in ethanol and n-hexane to study their fluorescence or their surface behavior at the air/water interface.

2.3 Characterization of ZnO Qdots

2.3.1 X-ray diffraction

X-ray diffraction (XRD) study was carried out to investigate the crystal structure of our Qdots and ensure there was not acetate, sodium ions or another contaminant. The XRD pattern was collected in the step scan mode with a small grazing angle of incident X-rays with a 2θ scan range of 5-80° and a step size of 0.02°.

2.3.2 Dynamic light scattering

Dynamic light scattering (DLS) measurements were taken in a Zetasizer Nano equipment. Samples were suspended in ethanol and sonicated 1 minute before measurments. Autocorrelation functions of 10 s data collection time per scan were averaged and evaluated by the Dispersion Technology Software (DTS) appendant to Zetasizer Nano. Calculation of hydrodynamic particle size was made using the cumulant analysis and multimodal size distribution algorithm that DTS includes. Every sample was measured 5 times and the reported value is the average.

2.3.3 Preparation and Characterization ZnO@ODS nanoparticle layers at the air/water interface

To be deposited in the air/water interface, ZnO@ODS Qdots were dispersed in hexane (99.99%, Aldrich) at a concentration of 1 mg/mL and ZnO Qdots were dispersed in ethanol (99.5%, Meyer). The dispersions were sonicated for 1 min, just before each experiment, using an ultrasonic bath (Fisher Scientific) to break particle aggregates. Compression isotherms were recorded on a Langmuir trough (Nima, area A = 243 cm^2) equipped with a Du Noüy-Padday platinum rod of 1.056 mm in diameter, for monitoring the surface tension. Before each experiment, Du Noüy-Padday rod was carefully washed with chloroform and thereafter flamed. The sub phase was ultrapure water from a Milli-Q instrument (Millipore). The trough was also cleaned with chloroform and ethanol before each experiment. Before spreading the Qdots in the Langmuir through, the surface of pure water was compressed and it was checked that the surface pressure did not exceed 0.3mN/m during the compression, ensuring the absence of contamination surface-active impurities. Particle layers were formed by spreading 300 μL of a dispersion of 1 mg/mL Qdots in hexane onto the water sub phase using a 1mL glass micro-syringe (Hamilton). The compression of the layer was started 20 min after spreading, ensuring solvent evaporation. Each isotherm presented is the resulting average of three experiments. All of the experiments were done at the of 20 ± 1 ℃, controlled with a refrigerated/heated bath circulator (HAAKE A10, Thermo scientific).

2.3.4 Continuous compression

In this series of experiments, the barriers were moved continuously to compress the layer. Two different barrier speeds were used here: 5 mm^2/min and

50 mm^2/min. During each continuous compression experiment, the barrier speed was kept constant.

2.3.5 Hysteresis cycles

In the experiments for studying hysteresis, the compression of the layers was immediately followed by an expansion at the same velocity.

3 Results and discussion

3.1 Crystalline structure and size of ZnO Qdots

The synthesis of the ZnO Qdots was conducted under controlled conditions by a sol-gel process from Zn acetate (Sigma) and NaOH, setting a constant temperature and controlling the ratio of dripping of the OH$^-$ solution into the Zn^{2+} solution during synthesis. Fig. 1 shows the XRD spectrum from one of our synthesized ZnO Qdot samples and the corresponding bulk ZnO pattern referenced in the open database RUFF (RRUFF ID: R050419). All XRD peaks of our sample correspond well with the referenced pattern in database, confirming the well formation of hexagonal ZnO crystal structures. No diffraction peaks from Zn(OH)$_2$ were found in the XRD spectrum. The line broadening observed in the diffraction peaks interpreted as a result of reduction in the crystalline size.

The average diameter of the Qdots was calculated using the Scherrer formula(West, 1984):

$$D = \frac{0.9\lambda}{B\cos\theta_B},\qquad(1)$$

where D is the particle size, λ is the X-ray wavelength and B is the full width at half maximum (FWHM) of the peak centered in θ_B, founding a value of 14.8 nm.
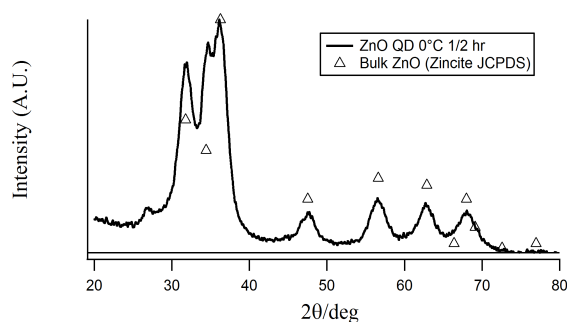

Fig. 1. XRD spectrum of ZnO Qdots from the hexagonal phase of ZnO.

The calculated value of 14.8 nm correspond to the primary particle diameter in their powder form, even though, from the dynamic light scattering measurements of our samples,in was found that the particles in suspension form stable aggregates with an average hydrodynamic radius of 121 ± 3.1 nm.

3.2 Surface properties of ZnO@ODS nanoparticles at the air/water interface

The interfacial properties of the ZnO@ODS nanocomposites with intermediate hydrophobicites were studied. For this purpose, the technique of the Langmuir trough was used to obtain the surface pressure Π vs surface density Γ isotherms as shown in Fig. 2, obtained at a constant compression rate, Where Π is the difference between the surface tension before and after spreading, and Γ is the surface covered by the particles, given as mass per unit area. Each point is the average of three different experiments. For the more hydrophobic particles studied, (ZnO4%ODS), it is noticed a fast increment in the surface pressure, even in small surface densities (Γ < 10 mg/m^2), a characteristic behavior of a condensed phase. For surface concentrations of Γ > 10 mg/m^2, it is observed a change in the slope, being more slow the increment of surface pressure with respect to the concentration, but there is no abrupt collapse of the layer. For the particles with intermediate hydrophobicity (ZnO2%ODS), it is observed a linear increment in the surface pressure in densities, in the range 13 < Γ < 15 mg/m^2, this linear behavior is characteristic of a liquid expanded phase. Next, in the point of Γ = 15 mg/m^2, it is observed a change in the slope of the isotherm, followed by a rapid increment of the surface pressure in the interval of 15 < Γ < 20 mg/m^2. There is no presence of any plateau region between the region with linear increment and the region with a fast increment; this meaning that there are no indicatives of a first order transitions between phases. For surface concentrations of Γ > 20 mg/m^2, it is noticed a semi constant region with a low value of interfacial tension. This layer does not collapse, rather than, the semi constant pressure remains while the barriers are getting closer. This behavior is similar to that reported previously on silica particle layers (Safouane *et al.*, 2007; D. Zang *et al.*, 2010; D. Y. Zang *et al.*, 2010), and is an indicative that these particles have high adsorption energies, so that, there is no collapse at higher pressures, due to the high amount of energy needed to desorb the particles from the surface.
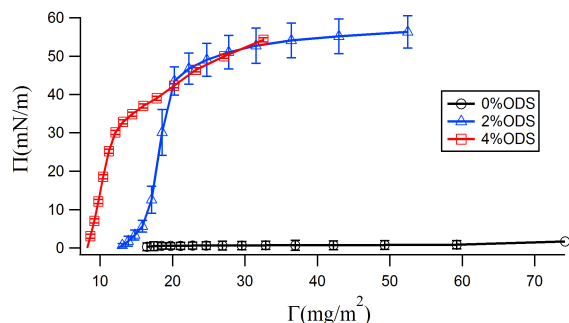
Fig. 2. Surface pressure vs surface density during the first compression for different particle hydrophobicities (given as % ODS). The rate of compression is 5 mm^2/min.

For the particles with less hydrophobicity (ZNO with 0%ODS), there is a small constant reduction in the surface tension of the air/water interface with an increment in the surface pressure, reaching a maximum value at $\Pi = 1.7$ mN/m, this behavior is due to ZnO nanoparticles are more soluble in water and they can desorb from the air/water surface with low amounts of energy.

The adiabatic compression modulus at equilibrium E_0 can be obtained from the slope of the isotherms, as:

$$E_0 = -A\frac{d\Pi}{dA} \qquad (2)$$

where A is the average available area per particle. In this case, it is dealing with the surface concentration Γ, which is inversely proportional to A, so that the expression for the modulus is:

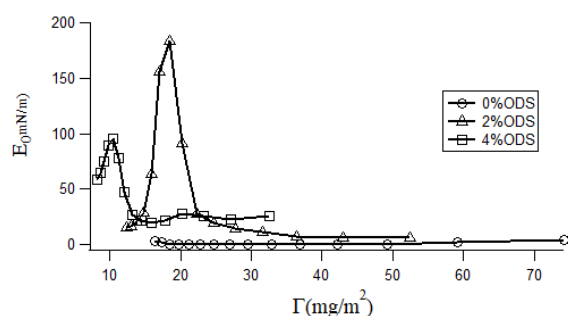$$E_0 = \Gamma\frac{d\Pi}{d\Gamma} \qquad (3)$$

Fig. 3. Static compression modulus E_0 as a function of the surface density for different particle hydrophobicities (given as % ODS). The rate of compression is 5 mm^2/min.

The adiabatic compression modulus curves are shown in fig. 3. The obtained modules showed different behavior for the different hydrophilicities studied. For pure ZnO (ZnO@0%ODS), the compression modulus reaches a low value ($E_0 < 3.5$ mN/m). The layer formed by the ZnO@2%ODS presented a maximum of their compression modulus at 183.5 mN/m, at the surface concentration of $\Gamma = 18.5$ mg/m^2. This value of E_0 corresponds to a liquid condensed phase. For the more hydrophobic nanoparticles (ZnO@4%ODS), the compression modulus had the maximum value of 95.5 mN/m, corresponding also to a liquid condensed phase, at a surface concentration of $\Gamma = 10.5$ mg/m^2. It is noticed that the layer made with more hydrophobic particles reach their maximum E_0 value in a lower surface concentration than those with intermediate hydrophobicity but, it is more compressible as their maximum E_0 value is smaller than for the ZnO@2%ODS. It means that the more hydrophobic particles produce a high reduction in the surface tension at smaller concentrations, but, they do not form a rigid layer, maybe due to a softened of the particles with the surface functionalization using silane.

Hysteresis of the layers of nanoparticles with intermediate hydrophobicity (ZnO@2% ODS) was studied. Significant hysteresis is observed between the first compression and expansion and also between the first expansion and the second compression as shown in Fig. 4. This result shows that the densification and packing of the layer is irreversible.
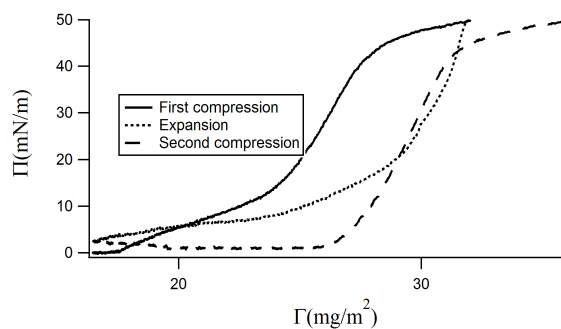

Fig. 4. Surface pressure-area ($\Pi - \Gamma$) isotherms of layers of Qdots with intermediate hydrophobicity (ZnO@2%ODS) recorded during the first and second compression-expansion cycles. The rate of compression (expansion) is 5 mm^2/min. The second cycle started immediately after the first one.
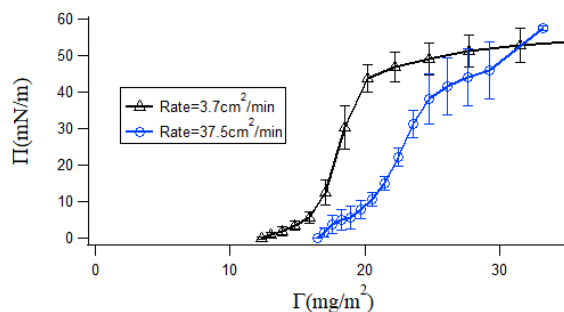
Fig. 5. $\Pi - \Gamma$ isotherms of the ZnO@ODS2% nanoparticle layers under two different rates of continuous compression
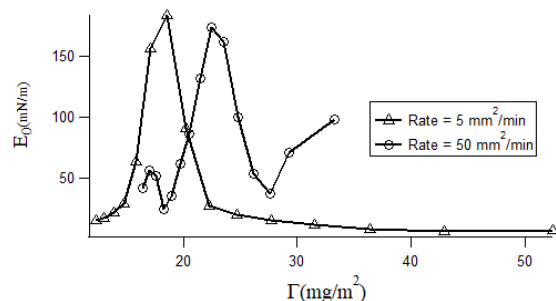

Fig. 6. Static compression modulus E_0 as a function of the surface density for of the ZnO@ODS2% nanoparticle layers under two different rates of continuous compression.

The influence of the compression rate on the isotherms profile was evaluated for the ZnO@2%ODS nanoparticles. As shown in Fig. 5, the layer starts to increase the surface pressure at higher concentrations when the barriers speed is incremented. From the compression modulus, shown in Fig. 6, it is observed that when the rate of compression is high, the layer becomes more compressible, since the maximum value of the modulus is lower than for the slow compression, an indicative of an extensional thinning behavior, i.e., rapid deformations leads to a softened of the layer. This result shows the complex, time dependent behavior of the layer and from them, it is expected a viscoelastic behavior with frequency-dependent modules under rheological experiments.

Conclusions

In this work, the first study of the interfacial mechanical properties of two dimensional layers formed by functionalized ZnO nanoparticles at the air/water interface at equilibrium is presented. Nanoparticles with partially hydrophobicity form soft solids, when they are compressed above concentrations of the order of 1×10^1 mg/mL, reaching values of their adiabatic compression modulus corresponding to a liquid condensed phase. Layers do not present collapse, rather than, a semi constant pressure value remains at higher surface concentrations, while the barriers are getting closer, an indicative of high adsorption energies. There was no evidence of first order transitions between the expanded to condensed phases. Nanoparticle layers presented a strong dependence with the rate of compression, an indicative that their viscoelastic parameters could be time dependent under dynamic rheology experiments. These results, among the presence of significant hysteresis on compression-expansion cycles, are evidence of the complex mechanical behavior of the two dimensional layers. The mechanical properties observed in the functionalized ZnO layers, make them suitable to be used as foam stabilizers, by their high adsorption energy, and their capacity to reduce the surface tension using low surface concentrations, remaining as a soft compressible material, able to dissipate the surface flow that tends to destabilize the foam structures.

Nomenclature

ZnO	Zinc Oxide
ODS	trimethoxy(octadecyl)silane.
ZnO@ODS	ZnO nanoparticles covered with trimethoxy(octadecyl)silane.

Symbols

Π	Surface pressure (mN/m).
Γ	Surface density (mg/m^2).
E_0	Adiabatic compression modulus at equilibrium (mN/m).
A	Average available area per particle.

References

Alshehri, N. A., Lewis, A. R., Pleydell-Pearce, C., & Maffeis, T. G. G. (2017). Investigation of the growth parameters of hydrothermal ZnO nanowires for scale up applications. *Journal of Saudi Chemical Society*. https://doi.org/10.1016/j.jscs.2017.09.004

Arriaga, L. R., Drenckhan, W., Salonen, A., Rodrigues, J. A., Íñiguez-Palomares, R., Rio, E., & Langevin, D. (2012). On the long-term stability of foams stabilised by mixtures of nano-particles and oppositely charged short chain surfactants. *Soft Matter 8*, 11085. https://doi.org/10.1039/c2sm26461g

Aveyard, R., Binks, B. P., & Clint, J. H. (2003). Emulsions stabilised solely by colloidal particles. *Advances in Colloid and Interface Science 100-102(SUPPL.)*, 503-546. https://doi.org/10.1016/S0001-8686(02)00069-6

Bang, J., Yang, H., & Holloway, P. H. (2006). Enhanced and stable green emission of ZnO nanoparticles by surface segregation of Mg. *Nanotechnology 17*, 973-8. https://doi.org/10.1088/0957-4484/17/4/022

Beneventi, D., Carre, B., & Gandini, A. (2001). Role of surfactant structure on surface and foaming properties. *Colloids and Surfaces A: Physicochemical and Engineering Aspects 189*, 65-73.

Benhebal, H., Chaib, M., Salmon, T., Geens, J., Leonard, A., Lambert, S. D., … Heinrichs, B. (2013). Photocatalytic degradation of phenol and benzoic acid using zinc oxide powders prepared by the sol-gel process. *Alexandria Engineering Journal 52*, 517-523. https://doi.org/10.1016/j.aej.2013.04.005

Bera, D., Qian, L., Sabui, S., Santra, S., & Holloway, P. H. (2008). Photoluminescence of ZnO quantum dots produced by a sol-gel process. *Optical Materials 30*, 1233-1239. https://doi.org/10.1016/j.optmat.2007.06.001

Binks, B. P. (2002). Particles as surfactants - Similarities and differences. *Current Opinion in Colloid and Interface Science 7*, 21-41.

https://doi.org/10.1016/S1359-0294(02)00008-0

Cervantes Martinez, A., Rio, E., Delon, G., Saint-Jalmes, A., Langevin, D., & Binks, B. P. (2008). On the origin of the remarkable stability of aqueous foams stabilised by nanoparticles: link with microscopic surface properties. *Soft Matter 4*, 1531. https://doi.org/10.1039/b804177f

Dickinson, E. (2010). Food emulsions and foams: Stabilization by particles. *Current Opinion in Colloid and Interface Science 15*, 40-49. https://doi.org/10.1016/j.cocis.2009.11.001

Du, Z., Bilbao-Montoya, M. P., Binks, B. P., Dickinson, E., Ettelaie, R., & Murray, B. S. (2003). Outstanding stability of particle-stabilized bubbles. *Langmuir 19*, 3106-3108. https://doi.org/10.1021/la034042n

El Filali, B., Torchynska, T. V., Díaz Cano, A. I., & Morales Rodríguez, M. (2015). Structural and Raman scattering studies of ZnO Cu nanocrystals grwn by spray pyrolysis. *Rev. Mex. Ing. Quím. 14*, 781-788.

Gonzenbach, U. T., Studart, A. R., Tervoort, E., & Gauckler, L. J. (2006). Ultrastable particle-stabilized foams. *Angewandte Chemie - International Edition 45*, 3526-3530. https://doi.org/10.1002/anie.200503676

Hunter, T. N., Pugh, R. J., Franks, G. V., & Jameson, G. J. (2008). The role of particles in stabilising foams and emulsions. *Advances in Colloid and Interface Science 137*, 57-81. https://doi.org/10.1016/j.cis.2007.07.007

Jana, N. R., Yu, H., Ali, E. M., Zheng, Y., & Ying, J. Y. (2007). Controlled photostability of luminescent nanocrystalline ZnO solution for selective detection of aldehydes. *Chemical Communications (Cambridge, England) 14*, 1406-1408. https://doi.org/10.1039/b613043g

Khan, J., Ilyas, S., Akram, B., Ahmad, K., Hafeez, M., Siddiq, M., & Ashraf, M. A. (2018). Zno/NiO coated multi-walled carbon nanotubes for textile dyes degradation. *Arabian Journal of Chemistry*. https://doi.org/10.1016/j.arabjc.2017.12.020

Kołodziejczak-Radzimska, A., & Jesionowski, T. (2014). Zinc Oxide−From Synthesis to

Application: A Review. *Materials 7*, 2833-2881. https://doi.org/10.3390/ma7042833

Lavand, A. B., & Malghe, Y. S. (2018). Synthesis, characterization and visible light photocatalytic activity of carbon and iron modified ZnO. *Journal of King Saud University - Science 30*, 65-74. https://doi.org/10.1016/j.jksus.2016.08.009

Li, S., Sun, Z., Li, R., Dong, M., Zhang, L., Qi, W., … Wang, H. (2015). ZnO Nanocomposites Modified by Hydrophobic and Hydrophilic Silanes with Dramatically Enhanced Tunable Fluorescence and Aqueous Ultrastability toward Biological Imaging Applications. *Scientific Reports 5*, 8475. https://doi.org/10.1038/srep08475

Lv, Y., Xiao, W., Li, W., Xue, J., & Ding, J. (2013). Controllable synthesis of ZnO nanoparticles with high intensity visible photoemission and investigation of its mechanism. *Nanotechnology 24*, 175702. https://doi.org/10.1088/0957-4484/24/17/175702

Mahmud, S., Abdullah, M. J., Putrus, G. A., Chong, J., & Mohamad, A. K. (2006). Nanostructure of ZnO fabricated via French process and its correlation to electrical properties of semiconducting varistors. *Synthesis and Reactivity in Inorganic, Metal-Organic and Nano-Metal Chemistry 36*, 155-159. https://doi.org/10.1080/15533170500524462

Miller, R., Joos, P., & Fainerman, V. B. (1994). Dynamic surface and interfacial tensions of surfactant and polymer solutions. *Advances in Colloid and Interface Science 49(C)*, 249-302. https://doi.org/10.1016/0001-8686(94)80017-0

Morkoç, H., & Özgür, U. (2009). *Zinc Oxide: Fundamentals, Materials and Device Technology. Structure*. Weinheim: WILEY-VCH verlag GmbH & Co. https://doi.org/10.1002/9783527623945.ch1

Olivarez-Romero, R., Faustino-vega, A., E., M.-C. J., González-Vázquez, R., & Azaola-Espinosa, A. (2018). Microencapsulation of Lactobacillus acidophilus LA-5 increases relative survival under simulated gastrointestinal tract stress. *Revista Mexicana de Ingeniera Qumica 17*, 641-650.

Özgür, Ü., Alivov, Y. I., Liu, C., Teke, A., Reshchikov, M. A., Doğan, S., … Morkoç, H. (2016). A comprehensive review of ZnO materials and devices. *Journal of Applied Physics 41301(2005)*, 1-102. https://doi.org/10.1063/1.1992666

Pavón-García, L. M. ., C., P. A., Rodríguez-Huezo, M. E., Jiménez-Alvarado, R., Alamilla Beltrán, L., & Román Guerrero, A. (2014). Effect of gelled inner aqueous phase rheology on the color degradation of muitle aqueous extracts incorporated into water-in-oil-in-water double emulsions. *Revista Mexicana de Ingeniería Química 13*, 665-677. https://doi.org/CC BY-NC 3.0

Perez, J., Barrios, E., Roman, A., & Pedroza, R. (2011). Interaction of mesquite gum-chitosan at the interface and its influences on the stability of multiple emulsions w1/O/w2. *Revista Mexicana de de Ingeniería Química 10*, 487-499.

Pickering, S. U. (1907). Emulsions. *Journal of the Chemical Society 91*, 2001-2021.

Rodríguez-Huezo, M. E., Villagcheómez-Zavala, D. L., Lozano-Valdés, B., & Pedroza-Islas, R. (2010). Surface properties of mize, fish and bovine serum protein hydrolysates. *Revista Mexicana de Ingeniera Qumica 9*, 241-250.

Safouane, M., Langevin, D., & Binks, B. P. (2007). Effect of particle hydrophobicity on the properties of silica particle layers at the air-water interface. *Langmuir 23*, 11546-11553. https://doi.org/10.1021/la700800a

Stocco, A., Garcia-Moreno, F., Manke, I., Banhart, J., & Langevin, D. (2011). Particle-stabilised foams: structure and aging. *Soft Matter 7*, 631-637. https://doi.org/10.1039/C0SM00166J

Van Dijken, A., Meulenkamp, E. A., Vanmaekelbergh, D., & Meijerink, A. (2000). Identification of the transition responsible for the visible emission in ZnO using quantum size effects. *Journal of Luminescence 90*, 123-128. https://doi.org/10.1016/S0022-2313(99)00599-2

West, A. R. (1984). *Solid State Chemistry and its Application*. New York: Wiley.

Zang, D., Langevin, D., Binks, B. P., & Wei, B. (2010). Shearing particle monolayers: Strain-rate frequency superposition. *Physical Review E - Statistical, Nonlinear, and Soft Matter Physics 81*, 1-5. https://doi.org/10.1103/PhysRevE.81.011604

Zang, D. Y., Rio, E., Langevin, D., Wei, B., & Binks, B. P. (2010). Viscoelastic properties of silica nanoparticle monolayers at the air-water interface. *European Physical Journal E 31*, 125-134. https://doi.org/10.1140/epje/i2010-10565-7